Domain gain or loss in fungal chitinases drives ecological specialization toward antagonism or immune suppression

Ruben Eichfeld[1,2], Asmamaw B. Endeshaw[1], Margareta J. Hellmann[3], Bruno M. Moerschbacher[3], Alga Zuccaro[1,2*]

[1]University of Cologne, Institute for Plant Sciences, Cologne, Germany

[2]Cluster of Excellence on Plant Sciences (CEPLAS), Cologne, Germany

[3]University of Münster, Institute of Biology and Biotechnology of Plants, Münster, Germany

*Correspondence: azuccaro@uni-koeln.de

Abstract

The evolutionary origins of fungal effector proteins remain poorly understood, particularly how structural changes reprogram antimicrobial enzymes into host-adapted immune suppressors. Here, we show that domain modularity drives ecological specialization in chitinase effectors of the beneficial root endophyte *Serendipita indica*. The GH18 chitinase *Si*CHIT, which carries a C-terminal carbohydrate-binding module (CBM5), is expressed during fungal competition and antagonizes the fungal pathogen *Bipolaris sorokiniana* in the rhizosphere, thereby protecting plant roots. Deletion of the CBM5 abolishes this antifungal activity, while fusion of CBM5 to the CBM5-lacking paralog *Si*CHIT2 restores pathogen inhibition. In contrast, *Si*CHIT2 is induced during root colonization and suppresses chitin-triggered reactive oxygen species production, promoting immune evasion and host compatibility. These results identify CBM5 as a modular determinant of effector function, switching chitinase activity between microbial antagonism and host immune suppression. Our findings support an evolutionary scenario

in which effector function in planta arises through domain loss and transcriptional divergence from an antimicrobial precursor, consistent with transitions along the saprotrophy-to-symbiosis continuum.

Significance Statement

Effector proteins play key roles in shaping fungal interactions with both plant hosts and microbial competitors, yet how these functions evolve remains unclear. Here, we show that structural domain modularity enables ecological specialization of two paralogous chitinases arising from gene duplication in the root endophyte *Serendipita indica*. Through domain deletion and fusion, we demonstrate that a carbohydrate-binding module (CBM5) determines whether a chitinase functions in microbial antagonism or immune evasion. Our findings provide mechanistic evidence for effector diversification via domain loss and transcriptional divergence, supporting an evolutionary trajectory from antimicrobial activity to host adaptation. This work advances our understanding of how modular architecture drives effector evolution and niche specialization in symbiotic fungi.

Highlights

- Gain or loss of a CBM5 binding domain drives effector specialization between fungal antagonism and immune suppression
- CBM5 acts as a modular determinant enabling antifungal activity in the GH18 chitinase *Si*CHIT
- The CBM5-lacking paralog *Si*CHIT2 suppresses host immunity and promotes root colonization
- Functional divergence following gene duplication illustrates evolutionary repurposing of an antimicrobial enzyme into an immune-suppressive effector

Introduction

Mutualistic fungi are ecologically important members of the rhizosphere microbiome, where they support plant health and influence microbial community structure and function (Martin & Tan, 2025) This diverse group includes ectomycorrhizal and arbuscular mycorrhizal fungi, as well as beneficial root endophytes. Unlike mycorrhizal fungi, root endophytes often colonize plant roots without forming specialized symbiotic structures and, depending on the host and environmental context, can enhance plant performance by promoting nutrient uptake, water acquisition, and tolerance to environmental stress (Vandenkoornhuyse *et al.*, 2002; Dastogeer *et al.*, 2018; Mesny *et al.*, 2021; Mahdi *et al.*, 2022; Andreo-Jimenez *et al.*, 2023; Zhang *et al.*, 2024). These fungi exemplify the evolutionary plasticity of fungal lifestyles, flexibly occupying ecological niches along the saprotrophy-to-symbiosis continuum. To colonize plant roots and shape their niche, beneficial root endophytes must overcome two key challenges: evasion of host immunity and competition with microbial antagonists and plant pathogens, a process recently shown to be supported by synergistic interactions with bacterial members of the core microbiota (Mahdi *et al.*, 2022). Both immune evasion and microbial competition are mediated by secreted effector proteins. Effector-mediated immune evasion often involves the degradation or masking of microbe-associated molecular patterns (MAMPs), such as β-1,3/1,6-glucans and chitin, to prevent recognition by host pattern recognition receptors (Lahrmann & Zuccaro, 2012; Fesel & Zuccaro, 2016; Wawra *et al.*, 2016). In parallel, effectors can alter the microbiota composition by suppressing microbial competitors, a strategy well documented in plant pathogens (Snelders *et al.*, 2020; Snelders *et al.*, 2021) and increasingly recognized in mutualistic fungi.

The beneficial root endophyte *Serendipita indica* (*Si*), a member of the widespread fungal order Sebacinales (Basidiomycota), colonizes a broad range of host plants and is known for its ability to promote growth and suppress plant immunity while protecting the host from pathogens. Colonization is confined to the rhizoplane, epidermis, and cortex, and depends on an intact host immune system (Lahrmann *et al.*, 2015). In addition to its host-associated functions, *Si* exhibits strong antifungal activity in the rhizosphere, particularly against the pathogen *Bipolaris sorokiniana (Bs)*, the causal agent of spot blotch and root

rot in cereals (Sarkar *et al.*, 2019; Mahdi *et al.*, 2022; Eichfeld *et al.*, 2024). This antagonism is mediated by a GH18-CBM5 endochitinase (*Si*CHIT), whose catalytic activity restricts *Bs* growth and recapitulates the protective effect of *Si* in planta (Eichfeld *et al.*, 2024).

GH18 chitinases, found across all fungal phyla, cleave β-1,4-glycosidic bonds in chitin, a major structural component of fungal cell walls. These enzymes fulfill diverse roles in nutrient scavenging, hyphal remodeling, and fungal antagonism (Seidl, 2008; Chen *et al.*, 2020). Their catalytic activity depends on a conserved DxxDxDxE motif, which defines the substrate-assisted catalytic mechanism characteristic of this family (van Aalten *et al.*, 2001; Bußwinkel *et al.*, 2018). While some chitinase-derived effectors have lost enzymatic activity and evolved to sequester MAMPs (Fiorin *et al.*, 2018), others retain catalytic function and are functionally enhanced by accessory domains such as carbohydrate-binding modules (CBMs) (Limón *et al.*, 2001; Limón *et al.*, 2004; Monge *et al.*, 2018). These non-catalytic domains increase substrate affinity and specificity, particularly for crystalline or polymeric forms of chitin (Itoh *et al.*, 2006; Matroodi *et al.*, 2013). *Si*CHIT features a C-terminal CBM5 domain, a modular architecture found predominantly in bacteria and Basidiomycota but absent in Ascomycota, suggesting a lineage-specific evolutionary adaptation (Chen *et al.*, 2020; Eichfeld *et al.*, 2024). Here, we investigate the functional significance of CBM5 in *Si*CHIT and examine how domain architecture modulates effector activity, enabling a switch between microbial antagonism and immune evasion.

We show that the CBM5 domain is essential for the antifungal and plant-protective function of *Si*CHIT. This chitinase is expressed during fungal competition and antagonizes the pathogen *Bs* in the rhizosphere, thereby protecting plant roots. In contrast, its closely related paralog *Si*CHIT2 lacks CBM5 and is induced during root colonization. *Si*CHIT2 promotes evasion of chitin-triggered immunity, preventing the generation of host-derived reactive oxygen species. Through domain-swapping experiments, we demonstrate that CBM5 functions as a modular determinant that switches the ecological role of a chitinase from microbial antagonism to host immune suppression. Together, our findings support a model in which effector specialization emerges through gene duplication, domain loss,

110 and transcriptional divergence, reprogramming an antimicrobial enzyme into a host-
111 adapted immune effector.

112 Results

113 CBM5 enhances binding to crystalline chitin and fungal cell wall without altering
114 product specificity

115 To investigate the role of the C-terminal CBM5 domain in *Si*CHIT (PIIN_03543), we
116 generated three recombinant variants, all lacking their native signal peptides: full-length
117 *Si*CHIT, a catalytically inactive mutant (*Si*CHIT^{E196Q}), and a truncated version lacking the
118 CBM5 domain (*Si*CHIT^{-CBM5}), which retained the proline-rich linker. The truncated
119 construct was produced by excluding the final 141 bp from the coding sequence. All
120 recombinant proteins were purified via affinity chromatography and verified by SDS-
121 PAGE (Fig. S1).

122 We first assessed chitinase activity on insoluble crab shell chitin using thin-layer
123 chromatography (TLC) and by quantifying reducing sugars after 20 hours of incubation
124 (Fig. 1A, B). These assays, along with endpoint measurements on chitin azure (CA) (Fig.
125 1C), revealed no major differences between full-length *Si*CHIT and *Si*CHIT^{-CBM5}.
126 However, time-course experiments on CA showed that the presence of CBM5 enhanced
127 early hydrolysis (Fig. 1D), suggesting that the domain increases the reaction rate during
128 initial substrate engagement.

129 To evaluate whether CBM5 influences product outcome, we analyzed the hydrolysates of
130 colloidal chitin by mass spectrometry. Both *Si*CHIT and *Si*CHIT^{-CBM5} produced similar
131 oligomer profiles dominated by chitobiose (A2), indicating that CBM5 does not alter
132 product specificity (Fig. 1E). Notably, substantial amounts of partially deacetylated
133 products, such as A1D1 and A2D2, were also detected. This likely reflects the fact that
134 colloidal chitin is not fully acetylated; deacetylated regions may form stretches with higher
135 solubility and increased accessibility, leading to their preferential cleavage by the
136 enzymes. To assess whether CBM5 affects subsite preferences, we analyzed the
137 hydrolysis products of chitosans with defined degrees of acetylation (DA). *Si*CHIT^{-CBM5}

138 displayed the same requirement for an acetylated unit at the -1 subsite and no detectable
139 shifts at adjacent positions compared to *Si*CHIT, confirming that CBM5 does not influence
140 catalytic specificity (Fig. 1F; Eichfeld *et al*., 2024).

141 To determine the role of CBM5 in substrate interaction, we performed pull-down assays
142 using crab shell chitin, highly deacetylated chitosan, and lyophilized, protein-free *Bs*
143 mycelium. *Si*CHIT^{-CBM5} showed reduced binding to crab shell chitin compared to full-
144 length *Si*CHIT, while no difference was observed with chitosan, suggesting that CBM5
145 enhances binding specifically to acetylated, crystalline substrates (Fig. 1G). Binding to *Bs*
146 mycelium was also reduced in the absence of CBM5, indicating that the domain
147 contributes to cell wall targeting.

148 Together, these results show that while CBM5 is dispensable for full catalytic activity and
149 does not alter product specificity, it enhances early hydrolysis rates and substrate binding,
150 particularly to crystalline or fungal cell wall-like chitin. This suggests that CBM5 improves
151 functional efficiency under biologically relevant conditions, likely contributing to the role of
152 *Si*CHIT in microbial competition.

153 CBM5 is required for antifungal activity and plant protection

154 We previously demonstrated that *Si*CHIT restricts the growth of *Bs* and reduces its
155 colonization of plant roots through its chitinolytic activity (Eichfeld *et al*., 2024). However,
156 the specific contribution of the CBM5 domain to this antifungal function remained
157 unresolved. To test whether CBM5 is required for *Bs* inhibition, we incubated *Bs* spores
158 with the full-length *Si*CHIT, the catalytically inactive mutant *Si*CHIT^{E196Q}, the truncated
159 variant lacking CBM5 *Si*CHIT^{-CBM5}, or the empty vector control Ev. As expected, *Bs* spore
160 germination was significantly reduced in the presence of active *Si*CHIT, but not with
161 *Si*CHIT^{E196Q}. *Si*CHIT^{-CBM5} showed a similar lack of inhibitory effect as *Si*CHIT^{E196Q} and
162 had only a minimal effect compared to the Ev control (Fig. 2A).

163 We next examined whether the loss of antifungal activity translates into reduced
164 protection of host roots. *Bs* spores treated with the same chitinase variants were used to
165 inoculate the roots of the *Bs* host *Hordeum vulgare* (*Hv*). As previously shown, *Si*CHIT-
166 treated spores led to a significant reduction in *Bs* colonization, as measured by fungal

167 transcript levels in roots. In contrast, *Si*CHIT^{E196Q} and *Si*CHIT^{-CBM5} had no effect (Fig. 2B).
168 Correspondingly, only *Si*CHIT mitigated the reduction in root biomass caused by *Bs*
169 infection (Fig. 2C). To test whether this effect is conserved in other hosts, we repeated
170 the experiment using *Arabidopsis thaliana* (*At*). *Si*CHIT reduced *Bs* biomass and
171 preserved root elongation, while *Si*CHIT^{E196Q} did not. *Si*CHIT^{-CBM5} had a weak protective
172 effect, albeit significantly lower than the full-length enzyme. (Fig. S2.).

173 Together, these results demonstrate that both chitinase activity and the CBM5 domain are
174 required for *Si*CHIT's antifungal and plant-protective functions. The loss of protection
175 observed in the CBM5-lacking variant suggests that this domain contributes to cell wall
176 binding and is critical for effective niche defense.

177 A CBM5-lacking paralog, *Si*CHIT2, is transcriptionally specialized for host colonization

178 GH18-CBM5 chitinases are absent in Ascomycota but occur frequently in the
179 Agaricomycetes (Basidiomycota), where gene copy number varies across species with
180 different ecological lifestyles (Eichfeld *et al*., 2024). To better define the structural
181 requirements for antifungal activity in *Si*, we compared the four GH18 chitinases encoded
182 in the genome with respect to phylogenetic relationships, domain architecture, and
183 transcriptional regulation. Of the four, only *Si*CHIT harbors a CBM5 domain, whereas the
184 other three chitinases contain no additional domains besides the GH18 catalytic domain
185 (Fig. 3A). *Si*CHIT and its closest paralog *Si*CHIT2 (PIIN_03542) share the highest
186 sequence identity and form a distinct phylogenetic pair among the *Si* GH18 chitinases
187 (Fig. 3A; Supplementary Fig. S3). The catalytic DxxDxDxE motif located at the -1 subsite
188 is conserved across all four chitinases, suggesting that each is catalytically active (Fig.
189 3B). Despite this shared motif, the chitinases exhibit distinct structural features. *Si*CHIT2
190 retains an 86-amino-acid C-terminal linker but lacks a CBM5 domain. *Si*CHIT3
191 (PIIN_11727) lacks a predicted signal peptide, while *Si*CHIT4 (PIIN_07603) features
192 extended surface-exposed loops within the GH18 domain (Supplementary Table S1).
193 Taken together, *Si*CHIT and *Si*CHIT2 are more similar to each other in sequence,
194 structure, and genomic context than to the other chitinases in *Si*. Notably, they are located
195 adjacent in the genome (Fig. 3C). Their tandem organization, high sequence identity, and

196 absence of CBM5 in *Si*CHIT2 support a gene duplication event followed by structural
197 divergence through domain loss.

198 To assess structural similarity, we generated AlphaFold models (Jumper *et al.* 2021;
199 Mirdita *et al*. 2022) of both enzymes after removing the predicted signal peptides. The
200 models confirmed the overall structural conservation of the GH18 catalytic domain and
201 the presence of a C-terminal linker in *Si*CHIT2, but no CBM5 domain (Fig. 3D & E).

202 To examine transcriptional regulation, we analyzed RNA-seq data from Eichfeld *et al*.
203 2024 and found that *Si*CHIT and *Si*CHIT2 were the only chitinases significantly
204 upregulated in biotic contexts. *Si*CHIT was specifically induced during fungal
205 confrontation, while *Si*CHIT2 was induced during colonization of barley, *Brachypodium*
206 and *Arabidopsis*. In contrast, *Si*CHIT3 and *Si*CHIT4 were not transcriptionally activated
207 under any tested biotic conditions, including interactions with pathogenic fungi, beneficial
208 bacteria, or different plant hosts (Fig. 3F & G). To extend the RNA-seq findings, we
209 measured the expression of *Si*CHIT and *Si*CHIT2 by qPCR following confrontation with
210 *Bs* and six additional filamentous fungi representing the major fungal lineages
211 Ascomycota, Basidiomycota, and Mucoromycota. *Si*CHIT was induced in several of these
212 interactions, whereas *Si*CHIT2 expression remained low under all tested microbial
213 conditions (Fig. 3H). Additionally, both *Si*CHIT and *Si*CHIT2 were induced when *S. indica*
214 was grown on crab shell chitin as the sole carbon source (Fig. 3I).

215 Together, these findings suggest that *Si*CHIT2 evolved a distinct function from *Si*CHIT
216 following gene duplication. Their divergent domain architecture and expression profiles
217 indicate functional specialization, with *Si*CHIT adapted for fungal antagonism and
218 *Si*CHIT2 for host colonization.

219 Fusion of CBM5 reprograms *Si*CHIT2 for fungal antagonism

220 To test whether the CBM5 domain of *Si*CHIT is sufficient to confer antifungal activity, we
221 constructed a chimeric protein consisting of the GH18 catalytic domain of *Si*CHIT2 fused
222 to the proline-rich linker and CBM5 domain of *Si*CHIT (*Si*CHIT2^{+CBM5}). As a control, we
223 generated a second construct in which only the linker was fused to the GH18 domain of
224 *Si*CHIT2 (*Si*CHIT2^{+link}) (Fig. 4A). As observed for native *Si*CHIT and *Si*CHIT^{-CBM5}, the

225 presence of CBM5 did not affect endpoint chitinase activity on crab shell chitin or chitin
226 azure (Fig. 4B, C). However, only *Si*CHIT2^{+CBM5} suppressed *Bs* spore germination,
227 comparable to the effect of full-length *Si*CHIT. In contrast, *Si*CHIT2^{+link} showed no
228 inhibitory activity (Fig. 4D). Consistent with these results, both *Si*CHIT and *Si*CHIT2^{+CBM5}
229 reduced root growth inhibition in barley caused by *Bs*, and limited pathogen colonization.
230 In contrast, *Si*CHIT^{-CBM5} and *Si*CHIT2^{+link} had no measurable protective effect (Fig. 4E &
231 F).

232 These results demonstrate that fusing CBM5 to *Si*CHIT2 is sufficient to confer antifungal
233 activity, indicating that CBM5 acts as a modular domain enabling functional adaptation
234 toward microbial antagonism.

235 *Si*CHIT2 suppresses chitin-triggered immunity and facilitates root colonization by *S.* 236 *indica*

237 Given the distinct plant-induced expression profile of *Si*CHIT2, we hypothesized that this
238 chitinase contributes to immune evasion during root colonization. Previous studies have
239 shown that *Podosphaera xanthii* uses chitinase-like effectors to degrade immunogenic
240 chitin oligomers and suppress host defense responses (Martínez-Cruz *et al.*, 2021). To
241 test whether *Si* chitinases function similarly, we incubated immunogenic chitohexaose
242 (A6) with recombinant *Si*CHIT, *Si*CHIT2, their respective variants, or the Ev control at a
243 1:1 molar ratio. The resulting hydrolysates were applied to barley roots to measure
244 reactive oxygen species (ROS) production. ROS accumulation was completely abolished
245 when chitohexaose was pre-treated with either *Si*CHIT2^{+link} or *Si*CHIT^{-CBM5}. In contrast,
246 treatment with *Si*CHIT2^{+CBM5} or full-length *Si*CHIT resulted in only partial or no
247 suppression of ROS accumulation (Fig. 5A, B). An intermediate reduction in ROS
248 accumulation was observed when chitohexaose was pre-treated with *Si*CHIT^{E196Q}, likely
249 due to the inactive catalytic cleft sequestering a fraction of the chitohexaose. None of the
250 recombinant chitinases induced ROS when applied in the absence of chitohexaose (Fig.
251 S4).

252 To assess whether this immune suppression contributes to host colonization, we co-
253 inoculated *Si* with 20 μM of each recombinant chitinase and quantified fungal biomass in

254 barley roots at three days post-inoculation. *Si*CHIT2^{+link} significantly enhanced root
255 colonization, whereas the other chitinases did not (Fig. 5C). *Si*CHIT^{-CBM5} showed a slight
256 but non-significant trend toward increased colonization.

257 These results suggest that *Si*CHIT2's ability to suppress ROS depends on the absence
258 of CBM5, which may otherwise restrict access to soluble substrates and favor binding to
259 insoluble chitin. This immune-suppressive function, together with its host-specific
260 transcriptional induction, underscores a distinct role for *Si*CHIT2 compared to its CBM5-
261 containing paralog.

262 Discussion

263 Effector proteins are central to the ecological success of root-colonizing fungi, mediating
264 interactions not only with host plants but also with competing microbes. While traditionally
265 associated with immune suppression (Stergiopoulos & de Wit, 2009), fungal effectors are
266 now also recognized for their roles in inter-microbial competition. They facilitate the
267 acquisition and maintenance of ecological niches in the rhizosphere and on root surfaces,
268 thereby supporting fungal persistence and competitive advantage (Snelders *et al.*, 2020;
269 Gómez-Pérez *et al.*, 2023; Eichfeld *et al.*, 2024). These dual roles are not restricted to
270 pathogens; beneficial fungi such as *Si* employ similar strategies to persist in complex
271 microbial communities, maintain host compatibility, and defend their niche. This functional
272 versatility reflects broader evolutionary trends across the fungal kingdom, where
273 transitions from saprotrophy to symbiosis are accompanied by the repurposing of
274 ancestral traits to meet ecological demands.

275 Here, we show that *Si* encodes two closely related GH18 chitinases, *Si*CHIT and
276 *Si*CHIT2, that have diverged structurally and transcriptionally to perform distinct functions.
277 *Si*CHIT, which carries a C-terminal CBM5 domain, is expressed during fungal
278 confrontation and contributes to pathogen growth inhibition and plant protection. In
279 contrast, *Si*CHIT2, is induced during root colonization, and suppresses chitin-triggered
280 immune responses in the host (Fig. 5). This divergence possibly reflects an evolutionary
281 trajectory driven by gene duplication and domain loss, enabling *Si* to balance microbial
282 antagonism and host compatibility through modular effector specialization.

283 The importance of domain modularity in effector function is supported by previous studies
284 in *Trichoderma* spp., where the addition of substrate-binding domains such as CBM1 or
285 CBM18 increases their binding affinity for insoluble substrates and enhances antifungal
286 activity by improving proximity and substrate targeting (Limón *et al.*, 2001; Limón *et al.*,
287 2004). However, such effects can be masked *in vivo* by genome-wide redundancy in cell
288 wall-degrading enzymes and antimicrobial effectors. Using purified proteins, we
289 demonstrate that the CBM5 domain is critical for the antifungal activity of *Si*CHIT. Its
290 deletion abolishes fungal antagonism and its reintroduction into *Si*CHIT2 restores this
291 function. This is consistent with studies in bacterial chitinases, where CBM5 loss reduces
292 antifungal activity, likely due to impaired substrate binding (Tsujibo *et al.*, 2003; Itoh *et al.*,
293 2006). In our assays, CBM5 enhanced early hydrolysis rates and binding to crystalline
294 chitin and fungal cell wall, but did not affect overall catalytic activity or product profile. This
295 suggests a proximity-based enhancement mechanism, in which CBM5 anchors the
296 enzyme at the fungal cell wall. Unlike antimicrobial or agglutinating lectins such as WSC3,
297 a β-1,3-glucan-binding lectin from *S. indica* that agglutinates fungal cells independently
298 of enzymatic activity (Wawra *et al.*, 2019), CBM5 alone does not provide antifungal activity
299 which requires a catalytically active GH18 core. Some fungal pathogens employ
300 catalytically inactive chitinase effectors (e.g., *Mp*Chi in *Moniliophthora perniciosa*; Fiorin
301 *et al.*, 2018 or active chitinases (e.g., *Mo*Chia1 in *Magnaporthe oryzae*; Yang & Yu, 2019;
302 or EWCAs; Martínez-Cruz *et al.*, 2021) to suppress host immunity by sequestering or
303 degrading free chitin oligomers. Similarly, we show that both *Si*CHIT2 and *Si*CHIT^{-CBM5}
304 can suppress chitohexaose-induced ROS production. These findings suggest that CBM5
305 may hinder activity on soluble substrates not by altering catalytic specificity, but by limiting
306 access to short oligomers through spatial constraints. CBM5 domains are structurally
307 optimized for engaging extended, crystalline chitin surfaces via aromatic stacking and
308 hydrogen bonding (Kezuka *et al.*, 2006; Vaaje-Kolstad *et al.*, 2019). Accordingly, CBM5-
309 containing chitinases like *Si*CHIT likely localize to insoluble polysaccharides in fungal cell
310 walls, anchoring the enzyme to non-immunogenic material. Although such substrate
311 targeting could in principle restrict access to soluble MAMPs, this is unlikely in the ROS
312 assay, where only chitohexaose is present. A more plausible explanation is that CBM5
313 increases the rigidity or steric bulk of the protein, thereby reducing flexibility and limiting

314 productive interaction with short ligands. In contrast, CBM5-lacking variants such as
315 *Si*CHIT2 remain free to access and degrade free immunogenic chitin oligomers. This
316 suggests that suppression of host immunity may require a CBM5-free configuration
317 optimized for apoplastic MAMP degradation during root colonization. Such structural
318 neofunctionalization provides a plausible trajectory for the evolution of fungal effector
319 functions. Given the saprotrophic ancestry and facultative symbiotic lifestyle of *S. indica*,
320 *Si*CHIT likely evolved under selective pressure from fungal competitors, whereas
321 *Si*CHIT2 emerged as an immune-suppressive effector during the transition to a root-
322 associated niche. This represents a clear case of functional divergence driven by domain
323 loss and regulatory rewiring. By comparison, the *Verticillium dahliae* effector *Vd*AMP3
324 illustrates a different evolutionary strategy: co-opted from an ancestral antimicrobial
325 protein, it retains both its antimicrobial activity and core structural features while
326 functioning in microbiota manipulation in planta. Rather than undergoing major
327 neofunctionalization, *Vd*AMP3 shows how effectors can be repurposed for new ecological
328 roles with minimal structural change (Snelders *et al.*, 2021). This highlights the diversity
329 of evolutionary pathways by which fungal effectors adapt to changing environments.

330 Together, our findings show that domain gain and loss can reprogram effector proteins for
331 distinct roles. CBM5 serves as a modular determinant, switching GH18 chitinase activity
332 between microbial antagonism and immune suppression. This highlights how structural
333 modularity enables fungi to adapt effectors to the dual pressures of rhizosphere
334 competition and host interaction in symbiotic fungi.

335 Material and Methods

336 Plant and fungal materials

337 *Hordeum vulgare* (*Hv*, L. cv Golden Promise) and *Arabidopsis thaliana* (*At*, Col-0) were
338 used as plant hosts. *Hv* seeds were surface-sterilized in 6 % sodium hypochlorite for 1 h
339 under constant shaking and subsequently washed five times for 30 min in sterile water.
340 Seeds were germinated for four days on wet filter paper at 21 °C in the dark. Seeds of *At*
341 were surface-sterilized in 70 % ethanol for 10 min and 100 % ethanol for 7 min. *At* seeds
342 were placed on ½ MS medium (Murashige-Skoog medium including vitamins, pH 5.6)

343 containing 1 % sucrose and stratified for three days in the dark and 4 °C prior to
344 germination on a day-night cycle of 8/16 h at 22/18 °C, 60 % humidity and 125 µmol/m^2
345 light intensity for seven days. *Serendipita indica* (*Si*, DSM11827) and *Bipolaris*
346 *sorokiniana* (*Bs*, ND90Pr) were used as fungal species. *Si* was grown on CM medium
347 (Complete Medium, 1.5 % agar, Hilbert *et al*. 2012) at 28 °C for 28 days in the dark. *Si*
348 spores were harvested by adding sterile water and scraping the spores with a scalpel.
349 The suspension was filtered through a sterile miracloth filter and spores were centrifuged
350 at 2,000 x g. The supernatant was discarded and spores were washed three times in
351 water. *Bs* was grown on modified CM medium (Sarkar *et al.*, 2019) at 28 °C for 14 days
352 in the dark. *Bs* spores were harvested like *Si* spores but a Drigalski spatula was used to
353 scrape the spores instead of a scalpel.

354 Preparation of fungal inoculants and plant colonization

355 For the preparation of *Bs* inoculants, spores were harvested from 21-day old plates and
356 incubated with the respective recombinant proteins (10 µM in 50 mM phosphate buffer)
357 for 16 h at 28 °C in the dark. For the preparation of *Si* inoculants, spores were harvested
358 from 28-day old plates and were allowed to germinate overnight in sterile water at 28 °C.
359 Prior to plant root inoculation, the respective recombinant proteins were added to 20 µM
360 in 50 mM phosphate buffer. Spore mixtures were diluted to 5000 spores/mL for *Bs* and
361 500,000 spores/mL for *Si* to yield the final working inoculants. For inoculation of *At*, ten
362 sterile seven-day old seedlings were placed on solid 1/10 PNM (pH 5.6) plates (0.005 %
363 KNO_3, 0.005 % KH_2PO_4, 0.0025 % K_2HPO_4, 0.049 % $MgSO_4$, 0.00472 % $Ca(NO_3)_2$,
364 0.0025 % NaCl, 0.5 % (v/v) Fe-EDTA stock solution, 1.2 % Gelrite, pH 5.6. After
365 autoclaving, 10 mL 1 M MES pH 5.6 was added. The EDTA stock solution contains 2.78 %
366 $FeSO_4$ x 7 H_2O, 4.13 % Na_2EDTA x $2H_2O$). Concentrations are indicated in w/v if not
367 stated otherwise. The roots were treated with 1 mL of the respective inoculant and grown
368 on a day-night cycle of 8/16 h at 22/18 °C, 60 % humidity and 125 µmol/m^2 light intensity
369 for three days. The root elongation was quantified by measuring the difference root length
370 at the start of the inoculation and the end of the experiment at three days post inoculation
371 (dpi). Roots were washed with water and snap frozen in liquid nitrogen for further RNA
372 extraction. For inoculation of *Hv*, four sterile seedlings were placed in glass jars containing

373 solid 1/10 PNM medium (pH 5.6) and inoculated with three mL of the respective inoculant.
374 The inoculated plants were grown on a day-night cycle of 16/8 h at 22/18 °C and 60 %
375 humidity and a light intensity of 108 µmol/m^2 for three days. The root weight was
376 quantified at three dpi. Roots were washed in water and snap frozen for further RNA
377 extraction.

378 Preparation of fungal confrontations

379 For the preparation of fungal inoculants, liquid CM medium was inoculated with 500,000
380 spores/mL. For all other fungi, mycelium was scraped from plates and transferred to liquid
381 CM. All fungi were grown for six days at 28 °C and 120 rpm. The mycelium was blended
382 and re-suspended in fresh CM (Hilbert *et al*. 2012) and regenerated for another 24 h.
383 Regenerated mycelium was filtered through miracloth filters and washed thoroughly with
384 sterile milliQ water. Fungal mycelia were mixed in a 1:1 ratio and 1 g of mycelium was
385 streaked on PNM plates containing 15 % agar. After six days, the mycelia were harvested,
386 dried with tissue papers and snap frozen in liquid nitrogen.

387 Fungal spore germination

388 To quantify the *Bs* spore germination, isolated spores were resolved in liquid CM to a
389 concentration of 100,000 spores/mL and 100 µL were added to the wells of sterile Lab-
390 Tek 2 chamber slides with cover (VWR). 100 µL of the respective treatment (Ev control or
391 purified protein) were added to a final concentration of 10 µM. The germination rate of
392 spores was quantified 6 h after treatment.

393 RNA extraction from plant roots and qPCR

394 Plant materials were ground in liquid nitrogen and 1 mL of TRIzol reagent (Thermo
395 Fischer scientific) was added. Samples were vortexed for 20 sec until all material was
396 resolved. 200 µL chloroform were added and samples vortexed again. Samples were
397 centrifuged at 17,000 x g and 4 °C for 30 min and 500 µL of the upper aqueous phase
398 were transferred to 500 µL isopropanol. The nucleic acids were precipitated at -20 °C for
399 16 h and pelleted by centrifugation at 17,000 x g and 4 °C for 30 min. Pellets were
400 washed three times with 70 % ethanol diluted in DEPC water. Remaining DNA was
401 removed by adding 1 µL DNase1 (1 U/µL) in 3 µL DNase1 buffer (10 x) (Thermo Fischer

402 scientific) and 26 µL RNase-free water. Samples were incubated at 37 °C for 30 min.
403 DNase digest was stopped by heating to 70 °C for 5 min and subsequent precipitation
404 with 2 volumes isopropanol and ½ volume of 7.5 M ammonium acetate for 16 h at -20 °C.
405 Samples were washed twice with 70 % ethanol in DEPC water and resolved in 30 µL
406 RNase-free water. Concentrations were determined using a NanoDrop 2000c
407 spectrophotometer (Thermo Fischer Scientific).

408 1 µg of RNA was used for reverse transcription into cDNA (Thermo Fischer Scientific).
409 First, 1 µL of random hexamer and of oligo-dt oligomers were added and incubated at
410 65 °C for 5 min and subsequently placed on ice. 4 µL 5 x reaction buffer, 1 µL Riboblock
411 RNase inhibitor (20 U/µL), 2 µL 10 mM dNTPs and 2 µL MMLV reverse transcriptase were
412 added and samples were incubated at 42 °C for 1 h. cDNA synthesis was stopped by
413 heating to 70 °C for 5 min. qPCR was conducted using the primers listed in
414 Supplementary Table S2.

415 Cloning of chitinase expression vectors

416 The coding sequence (CDS) of the chitinase genes were amplified by PCR with Q5 High-
417 Fidelity Polymerase (New England Biolabs) using the primers listed in Supplementary
418 Table S2. PCR products were cloned using the Gibson assembly cloning technique into
419 the PQE80L expression vector (Qiagen, Hilden, Germany) after vector linearization with
420 Kpn1 (New England Biolabs).

421 Production and purification of recombinant protein in *E. coli*

422 Chemically competent *E. coli* BL21 cells were transformed with the vectors for protein
423 expression under control of a lac operon. 5 mL starter cultures were prepared in liquid LB
424 medium containing 100 µg/mL carbenicillin and grown for 16 h at 37 °C and 180 rpm.
425 Starter cultures were transferred to 300 mL of LB medium with carbenicillin and grown to
426 an OD_{600} of 0.5 at 28 °C. Gene expression was induced by adding IPTG to a final
427 concentration of 1 mM and cells were grown at 16 °C for 20 h. Cells were pelleted by
428 centrifugation at 5000 g for 15 min at 4 °C. Bacterial pellets were resolved in 5 mL lysis
429 buffer (50 mM NaH_2PO_4, 300 mM NaCl and 10 mM imidazole, pH 8) and sonicated three
430 times for 1 min with pulses on ice and centrifuged at 16,200 g for 30 min. 5 mL of the

431 supernatant were added to 1 mL of Nickel-NTA Agarose (Qiagen, Hilden, Germany) and
432 incubated under continuous shaking at 4 °C for 1 h. Samples were spun down at 500 g
433 for 10 secs, the flow through was removed, 4 mL wash buffer (50 mM NaH_2PO_4, 300 mM
434 NaCl and 20 mM imidazole, pH 8) were added and samples were incubated under
435 continuous shaking at 4 °C for 10 min. Washing steps were repeated five times. For
436 elution, 1 mL of elution buffer (50 mM NaH_2PO_4, 300 mM NaCl and 250 mM imidazole,
437 pH 8) was added and samples were incubated under continuous shaking at 4 °C for 10
438 min. Eluted fractions were dialyzed against 50 mM phosphate buffer (pH 6) over night
439 and protein concentrations were measured using Bradford reagent. To test the purity of
440 the protein samples, aliquots were boiled for 5 min in SDS-sample buffer, loaded on a 10
441 % SDS gel and visualized by Coomassie staining.

442 Chitinase activity assays

443 To quantify the enzymatic activity of the purified chitinases, 2 mg/mL chitin azure (Sigma
444 Aldrich) were incubated with 5 µM recombinant chitinase in a total volume of 200 µL.
445 Reactions were incubated at 28 °C for 20 h. Reactions were stopped by heating to 95 °C
446 for 5 min and samples were centrifuged 5 min at 17,000 x g and the absorbance of
447 supernatants was quantified at 560 nm. For quantifying reducing ends, 10 g crab shell
448 chitin were incubated with 5 µM enzyme in 200 µL 50 mM phosphate buffer for 20 h at
449 28 °C. Reactions were stopped by heating to 95 °C for 5 min. Samples were centrifuced
450 for 5 min at 17,000 x g and supernatant were mixed in a 1:1 ratio with DNSA (3,5-
451 dinitrosalicylic acid) reagent. DNSA reagent is prepared by mixing 1 % (w/v) 3,5-
452 dinitroslicylic acid, 1.6 % (w/v) sodium hydroxide, 30 % (w/v) potassium sodium tartrate
453 tetrahydrate. The samples were heated for 10 min at 95 °C and subsequently transferred
454 to ice. The absorbance of the samples was measured at 540 nm.

455 For TLC, 10 mg crab shell chitin (Sigma Aldrich) were weighed in 2 mL reaction tubes
456 and recombinant chitinases were added to a final concentration of 5 µM in 200 µL.
457 Reactions were incubated at 28 °C for 20 h and stopped by heating to 95 °C for 5 min.
458 Samples were centrifuged at 17,000 x g for 5 min. 10 µL of the supernatant were
459 separated on 60 F_{254} TLC (Sigma Aldrich) silica gel plates with running buffer (n-
460 butanol/methanol/28 % ammonium hydroxide/water, 5/4/2/1). Plates were dried and then

461 bathed in developer solution (1.6 g diphenylamine/1.6 mL aniline/12 mL 85 % phosphoric
462 acid/80 mL acetone). TLC plates were developed in an incubation oven at 100 °C for 20
463 to 30 min.

464 Chitinase subsite specificity

465 The subsite specificity of *Si*CHIT^{-CBM5} was determined as previously reported (Cord-
466 Landwehr *et al.*, 2017; Eichfeld *et al.*, 2024).

467 Substrate binding assay

468 15 mg of crab shell chitin (Sigma Aldrich), Chitosan (Sigma Aldrich) or freeze-dried
469 mycelium of *Bs* were weighed in a 2 mL reaction tube and incubated with 400 µL chitin-
470 binding buffer (2 mM KH_2PO_4, 8 mM Na_2HPO_4, 2 mM KCL) and 100 µL of 20 µM
471 recombinant protein shaking at 4 °C for 1 h. Samples were centrifuged at 17,000 x g for
472 5 min and 60 µL of the supernatant were mixed with 60 µL Bradford reagent. Protein
473 amounts were quantified at 595 nm and compared to the input amount.

474 Quantification of reactive oxygen species (ROS)

475 For elicitor preparation, 10 µM of chitohexaose were incubated with 10 µM of recombinant
476 chitinase or the buffer control for 16 h at 28 °C. Reactions were stopped by heating to
477 95 °C for 5 min and chitohexaose was diluted to 250 nM.

478 Four root pieces (0.5 cm) of four-day old barley seedlings were transferred to each well
479 of a 96-well microtiter plate (white, flat bottom) containing 200 µL of 2.5 mM 2-(N-
480 morpholino)ethanesulfonic acid (MES) buffer, pH 5.6. The plate was incubated for 16 h at
481 21°C for recovery. The buffer was replaced with 100 µL 2.5 mM MES buffer containing
482 20 µM LO-12 and 20 µg/mL Horseradish peroxidase (HRP). After 25-min incubation in the
483 dark, 100 µL of 250 nM chitohexaose elicitor solution was added to each well.
484 Chemiluminescence was measured using a TECAN SPARK 10 M microplate reader over
485 all wells for 2 h with an integration time of 450 ms.

Data availability

All data supporting the findings of this study are available within the article and supporting information.

Acknowledgements

We acknowledge support from the Cluster of Excellence on Plant Sciences (CEPLAS) funded by the Deutsche Forschungsgemeinschaft (DFG, German Research Foundation) under Germany's Excellence Strategy-EXC 2048/1-Project ID: 390686111 and the ZU 263/11-2 (SPP 2125 DECRyPT).

Competing interest

The authors declare no competing interest.

Author contributions

AZ and RE conceptualized the study. RE and AE conducted most of the research. MJH, BMM and RE conducted mass spectrometric analysis of the product profile and the subsite specificity. AZ and RE wrote the manuscript with input from all authors.

References

Andreo-Jimenez B, Te Beest DE, Kruijer W, Vannier N, Kadam NN, Melandri G, Jagadish SVK, van der Linden G, Ruyter-Spira C, Vandenkoornhuyse P, et al. 2023. Genetic Mapping of the Root Mycobiota in Rice and its Role in Drought Tolerance. *Rice (N Y)* **16**(1): 26.

Bußwinkel F, Goñi O, Cord-Landwehr S, O'Connell S, Moerschbacher BM. 2018. Endochitinase 1 (Tv-ECH1) from Trichoderma virens has high subsite specificities for acetylated units when acting on chitosans. *International Journal of Biological Macromolecules* **114**: 453-461.

Chen W, Jiang X, Yang Q. 2020. Glycoside hydrolase family 18 chitinases: The known and the unknown. *Biotechnology Advances* **43**: 107553.

Cord-Landwehr S, Ihmor P, Niehues A, Luftmann H, Moerschbacher BM. 2017. Quantitative Mass-Spectrometric Sequencing of Chitosan Oligomers Revealing Cleavage Sites of Chitosan Hydrolases. **89**(5): 2893-2900.

Dastogeer KMG, Li H, Sivasithamparam K, Jones MGK, Wylie SJ. 2018. Fungal endophytes and a virus confer drought tolerance to Nicotiana benthamiana plants through modulating osmolytes, antioxidant enzymes and expression of host drought responsive genes. *Environmental and Experimental Botany* **149**: 95-108.

518 **Eichfeld R, Mahdi LK, De Quattro C, Armbruster L, Endeshaw AB, Miyauchi S,**
519 **Hellmann MJ, Cord-Landwehr S, Peterson D, Singan V, et al. 2024.**
520 Transcriptomics reveal a mechanism of niche defense: two beneficial root
521 endophytes deploy an antimicrobial GH18-CBM5 chitinase to protect their hosts.
522 *New Phytologist* **244**(3): 980-996.
523 **Fesel PH, Zuccaro A. 2016.** β-glucan: Crucial component of the fungal cell wall and
524 elusive MAMP in plants. *Fungal Genetics and Biology* **90**: 53-60.
525 **Fiorin GL, Sanchéz-Vallet A, Thomazella DPT, do Prado PFV, do Nascimento LC,**
526 **Figueira AVO, Thomma B, Pereira GAG, Teixeira P. 2018.** Suppression of Plant
527 Immunity by Fungal Chitinase-like Effectors. *Curr Biol* **28**(18): 3023-3030.e3025.
528 **Gómez-Pérez D, Schmid M, Chaudhry V, Hu Y, Velic A, Maček B, Ruhe J, Kemen A,**
529 **Kemen E. 2023.** Proteins released into the plant apoplast by the obligate parasitic
530 protist Albugo selectively repress phyllosphere-associated bacteria. *New*
531 *Phytologist* **239**(6): 2320-2334.
532 **Hilbert M, Voll LM, Ding Y, Hofmann J, Sharma M, Zuccaro A. 2012.** Indole derivative
533 production by the root endophyte Piriformospora indica is not required for growth
534 promotion but for biotrophic colonization of barley roots. *New Phytologist* **196**(8):
535 520-534.
536 **Itoh Y, Watanabe J, Fukada H, Mizuno R, Kezuka Y, Nonaka T, Watanabe T. 2006.**
537 Importance of Trp59 and Trp60 in chitin-binding, hydrolytic, and antifungal
538 activities of Streptomyces griseus chitinase C. *Appl Microbiol Biotechnol* **72**(6):
539 1176-1184.
540 **Jumper J, Evans R, Pritzel A *et al*. 2021.** Highly accurate protein structure prediction
541 with AlphaFold. *Nature* **596**(8): 583-589.
542 **Kezuka Y, Ohishi M, Itoh Y, Watanabe J, Mitsutomi M, Watanabe T, Nonaka T. 2006.**
543 Structural Studies of a Two-domain Chitinase from Streptomyces griseus
544 HUT6037. *Journal of Molecular Biology* **358**(2): 472-484.
545 **Lahrmann U, Strehmel N, Langen G, Frerigmann H, Leson L, Ding Y, Scheel D,**
546 **Herklotz S, Hilbert M, Zuccaro A. 2015.** Mutualistic root endophytism is not
547 associated with the reduction of saprotrophic traits and requires a
548 noncompromised plant innate immunity. *New Phytologist* **207**(3): 841-857.
549 **Lahrmann U, Zuccaro A. 2012.** Opprimo ergo sum--evasion and suppression in the root
550 endophytic fungus Piriformospora indica. *Mol Plant Microbe Interact* **25**(6): 727-
551 737.
552 **Limón MC, Chacón MR, Mejías R, Delgado-Jarana J, Rincón AM, Codón AC, Benítez**
553 **T. 2004.** Increased antifungal and chitinase specific activities of Trichoderma
554 harzianum CECT 2413 by addition of a cellulose binding domain. *Applied*
555 *Microbiology and Biotechnology* **64**(5): 675-685.
556 **Limón MC, Margolles-Clark E, Benítez T, Penttilä M. 2001.** Addition of substrate-
557 binding domains increases substrate-binding capacity and specific activity of a
558 chitinase from Trichoderma harzianum. *FEMS Microbiology Letters* **198**(1): 57-63.
559 **Mahdi LK, Miyauchi S, Uhlmann C, Garrido-Oter R, Langen G, Wawra S, Niu Y, Guan**
560 **R, Robertson-Albertyn S, Bulgarelli D, et al. 2022.** The fungal root endophyte
561 Serendipita vermifera displays inter-kingdom synergistic beneficial effects with the
562 microbiota in Arabidopsis thaliana and barley. *The ISME Journal* **16**(3): 876-889.

Martin F, Tan H. 2025. Saprotrophy-to-symbiosis continuum in fungi. *Current Biology* **35**(11): R469-R475.

Martínez-Cruz J, Romero D, Hierrezuelo J, Thon M, de Vicente A, Pérez-García A. 2021. Effectors with chitinase activity (EWCAs), a family of conserved, secreted fungal chitinases that suppress chitin-triggered immunity. *The Plant Cell* **33**(4): 1319-1340.

Matroodi S, Motallebi M, Zamani M, Moradyar M. 2013. Designing a new chitinase with more chitin binding and antifungal activity. *World J Microbiol Biotechnol* **29**(8): 1517-1523.

Mesny F, Miyauchi S, Thiergart T, Pickel B, Atanasova L, Karlsson M, Hüttel B, Barry KW, Haridas S, Chen C, et al. 2021. Genetic determinants of endophytism in the Arabidopsis root mycobiome. *Nature Communications* **12**(1): 7227.

Mirdita M, Schütze K, Moriwaki Y, Heo L, Ovchinnikov S, Steinegger M. 2022. ColabFold: making protein folding accessible to all. *Nature Methods* **19**(6): 679-682.

Monge EC, Tuveng TR, Vaaje-Kolstad G, Eijsink VGH, Gardner JG. 2018. Systems analysis of the glycoside hydrolase family 18 enzymes from Cellvibrio japonicus characterizes essential chitin degradation functions. *J Biol Chem* **293**(10): 3849-3859.

Sarkar D, Rovenich H, Jeena G, Nizam S, Tissier A, Balcke GU, Mahdi LK, Bonkowski M, Langen G, Zuccaro A. 2019. The inconspicuous gatekeeper: endophytic Serendipita vermifera acts as extended plant protection barrier in the rhizosphere. *New Phytologist* **224**(2): 886-901.

Seidl V. 2008. Chitinases of filamentous fungi: a large group of diverse proteins with multiple physiological functions. *Fungal Biology Reviews* **22**(1): 36-42.

Snelders NC, Petti GC, van den Berg GCM, Seidl MF, Thomma BPHJ. 2021. An ancient antimicrobial protein co-opted by a fungal plant pathogen for in planta mycobiome manipulation. *Proceedings of the National Academy of Sciences* **118**(49): e2110968118.

Snelders NC, Rovenich H, Petti GC, Rocafort M, van den Berg GCM, Vorholt JA, Mesters JR, Seidl MF, Nijland R, Thomma BPHJ. 2020. Microbiome manipulation by a soil-borne fungal plant pathogen using effector proteins. *Nature Plants* **6**(11): 1365-1374.

Stergiopoulos I, de Wit PJGM. 2009. Fungal Effector Proteins. *Annual Review of Phytopathology* **47**(Volume 47, 2009): 233-263.

Tsujibo H, Kubota T, Yamamoto M, Miyamoto K, Inamori Y. 2003. Characterization of Chitinase Genes from an Alkaliphilic Actinomycete, Nocardiopsis prasina OPC-131. *Applied and Environmental Microbiology* **69**(2): 894-900.

Vaaje-Kolstad G, Tuveng TR, Mekasha S, Eijsink VGH 2019. Enzymes for Modification of Chitin and Chitosan. *Chitin and Chitosan*, 189-228.

van Aalten DM, Komander D, Synstad B, Gåseidnes S, Peter MG, Eijsink VG. 2001. Structural insights into the catalytic mechanism of a family 18 exo-chitinase. *Proc Natl Acad Sci U S A* **98**(16): 8979-8984.

Vandenkoornhuyse P, Baldauf SL, Leyval C, Straczek J, Young JPW. 2002. Extensive Fungal Diversity in Plant Roots. *Science* **295**(5562): 2051-2051.

608 **Wawra S, Fesel P, Widmer H, Neumann U, Lahrmann U, Becker S, Hehemann J-H,**
609 **Langen G, Zuccaro A. 2019.** FGB1 and WSC3 are in planta-induced β-glucan-
610 binding fungal lectins with different functions. *New Phytologist* **222**(3): 1493-1506.
611 **Wawra S, Fesel P, Widmer H, Timm M, Seibel J, Leson L, Kesseler L, Nostadt R,**
612 **Hilbert M, Langen G, et al. 2016.** The fungal-specific β-glucan-binding lectin
613 FGB1 alters cell-wall composition and suppresses glucan-triggered immunity in
614 plants. *Nature Communications* **7**(1): 13188.
615 **Yang C, Yu Y. 2019.** Binding of the Magnaporthe oryzae Chitinase MoChia1 by a Rice
616 Tetratricopeptide Repeat Protein Allows Free Chitin to Trigger Immune Responses.
617 **31**(1): 172-188.
618 **Zhang Y, Yang Z, Yang Y, Han A, Rehneke L, Ding L, Wei Y, Liu Z, Meng Y, Schäfer**
619 **P, et al. 2024.** A symbiont fungal effector relocalizes a plastidic oxidoreductase to
620 nuclei to induce resistance to pathogens and salt stress. *Current Biology* **34**(13):
621 2957-2971.e2958.

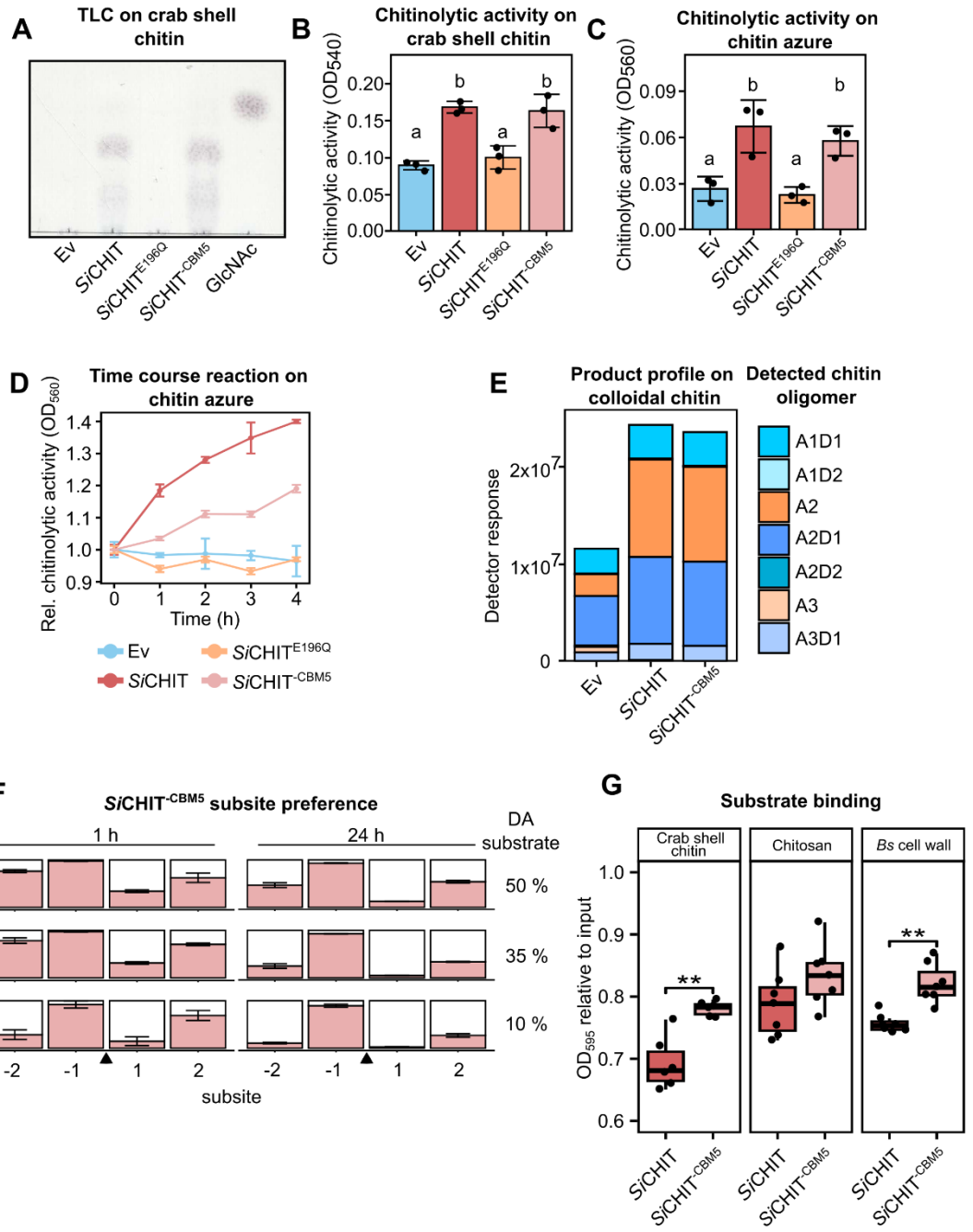

Figure 1: CBM5 enhances binding to fungal cell wall and crystalline chitin and promotes hydrolysis without affecting product specificity. A) Thin layer chromatography (TLC) of crab shell chitin incubated with the Ev control or 10 µM of *Si*CHIT, *Si*CHIT^{E196Q}, or *Si*CHIT^{-CBM5} at 28 °C for 20 h. **B)** Chitinase activity of recombinant chitinases on crab shell chitin at 10 µM and after 20 h at 28 °C. Samples were spun down and supernatants mixed 1:1 with DNSA reagent. Samples were incubated at 100 °C for 10 min and placed on ice. Subsequently, the relative amount of reducing ends was measured at 540 nm (mean +/- SD, n = 3). **C)** Chitinase activity of recombinant chitinases at 10 µM after 20 h at 28 °C on chitin azure (CA). Samples were spun down and supernatants were quantified at 560 nm (mean +/- SD, n = 3). **D)** Chitinase activity of recombinant chitinases at 10 µM measured over 4 h at 28 °C and normalized to the value of t_0 (mean +/- SEM, n = 3). **E)** Product profile of *Si*CHIT and *Si*CHIT^{-CBM} on colloidal chitin. Samples were incubated with

5 µM of chitinases for 24 h at 28 °C and hydrolysis products were identified and quantified via MS. A = acetylated, D = de-acetylated unit. **F)** Subsite preference of *Si*CHIT^{-CBM5} measured by MS. Chitosan of three degrees of acetylation (DA) were hydrolyzed for 1 h or 24 h. Based on the sequenced products, the frequency of acetylated units at the -2 to +2 subsites of *Si*CHIT^{-CBM5} was determined. The black arrow indicates the gylcosidic bond between the -1 and +1 subsite that is cleaved by the enzyme. **G)** Substrate-binding ability of *Si*CHIT and *Si*CHIT^{-CBM5} on crab shell chitin, > 75 % de-acetylated chitosan or lyophilized *Bs* mycelium. Binding was assessed by measuring the protein amount in the supernatant of reactions compared to input amount (n = 6-8). Limits of the boxplots represent the 25th–75th percentile, the horizontal line represents the median and the whiskers the minimum/maximum values without outliers. Statistical analysis: **B** and **D)** Different letters indicate significant differences according to one-way ANOVA followed by Tukey's HSD test (adjusted p-value < 0.05). **G)** Student's t-test (P-value: * < 0.05; ** < 0.01).

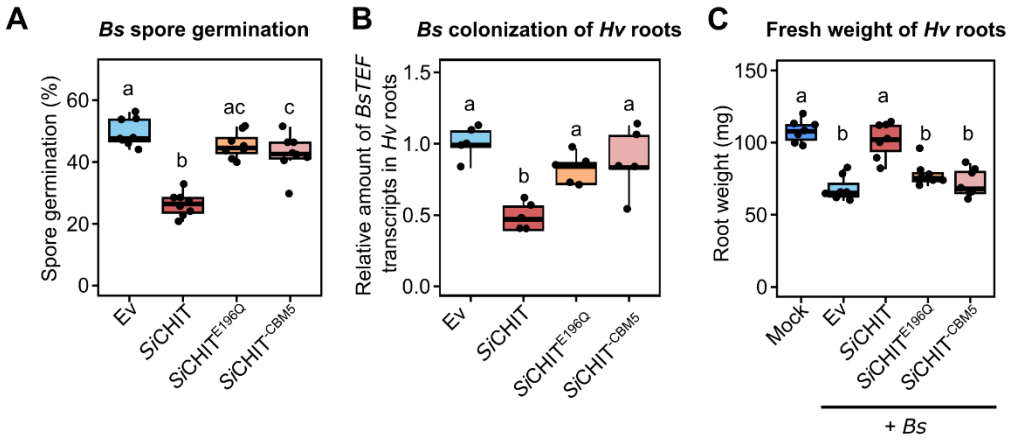

Figure 2: The CBM5 domain is essential for the antifungal and plant-protective activity of SiCHIT. A) Relative *Bs* spore germination six h post incubation in sterile chamber slides with the Ev control or 10 µM of *Si*CHIT, *Si*CHIT^{E196Q} or *Si*CHIT^{-CBM5} (n = 6). **B)** Colonization of *Hv* roots by *Bs* at three dpi inferred from relative expression of the fungal housekeeping gene *BsTEF* compared to the *Hv* housekeeping gene *HvUBI* inferred by qPCR using the $2^{-\Delta CT}$ method. Colonization values were normalized to the Ev control. *Bs* spores were either pre-treated with the Ev control or 10 µM of recombinant chitinases for 20 h at 28 °C (mean +/- SD, n = 4). **C)** *Hv* root fresh weight at three dpi with *Bs* spores. *Bs* spores were either pre-treated with the Ev control or 10 µM of recombinant chitinases for 20 h at 28 °C (n = 5-7). Limits of the boxplots represent the 25th–75th percentile, the horizontal line represents the median and the whiskers the minimum/maximum values without outliers. Statistical analysis: Different letters indicate significant differences according to one-way ANOVA followed by Tukey's HSD test (adjusted p-value < 0.05).

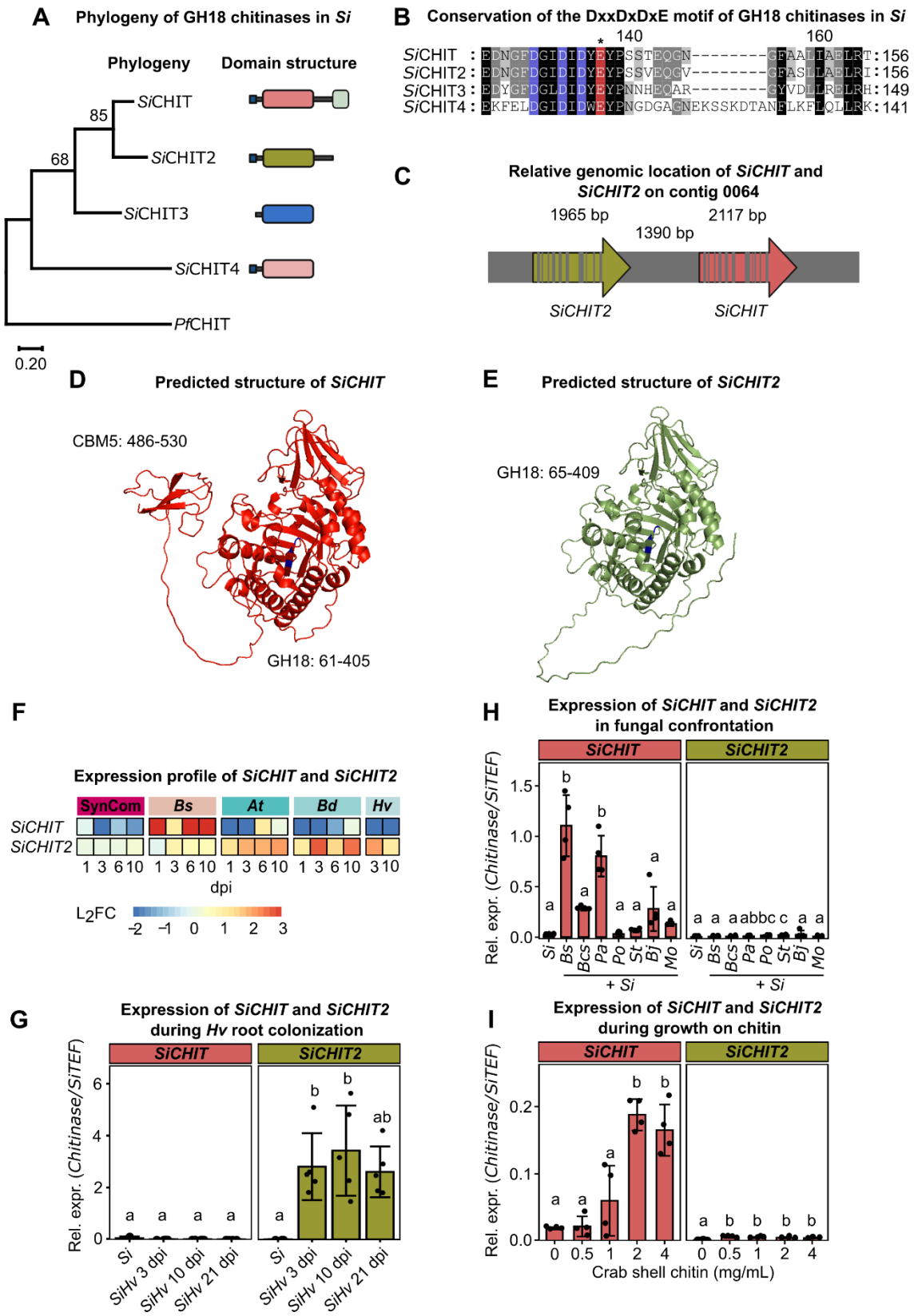
A
Phylogeny of GH18 chitinases in Si
Phylogeny
Domain structure
SiCHIT
SiCHIT2
SiCHIT3
SiCHIT4
PfCHIT
85
68
0.20
B
Conservation of the DxxDxDxE motif of GH18 chitinases in Si
140
160
SiCHIT : EDNGFDGIDIDYEYPSSTEQGN--------GFAALIAELRT:156
SiCHIT2 : EDNGFDGIDIDYEYPSSVEQGV--------GFASLLAELRI:156
SiCHIT3 : EDYGFDGLDIDYEYPNNHEQAR--------GYVDLLRELRH:149
SiCHIT4 : EKFELDGIDIDWEYPNGDGACNEKSSKDTANELKFLQLLRK:141
C
Relative genomic location of SiCHIT and SiCHIT2 on contig 0064
1965 bp
1390 bp
2117 bp
SiCHIT2
SiCHIT
D
Predicted structure of SiCHIT
CBM5: 486-530
GH18: 61-405
E
Predicted structure of SiCHIT2
GH18: 65-409
F
Expression profile of SiCHIT and SiCHIT2
SynCom
Bs
At
Bd
Hv
SiCHIT
SiCHIT2
1 3 6 10
dpi
L2FC
-2 -1 0 1 2 3
G
Expression of SiCHIT and SiCHIT2 during Hv root colonization
SiCHIT
SiCHIT2
Rel. expr. (Chitinase/SiTEF)
Si
SiHv 3 dpi
SiHv 10 dpi
SiHv 21 dpi
H
Expression of SiCHIT and SiCHIT2 in fungal confrontation
SiCHIT
SiCHIT2
Rel. expr. (Chitinase/SiTEF)
Si
Bs
Bcs
Pa
Po
St
Bj
Mo
+ Si
I
Expression of SiCHIT and SiCHIT2 during growth on chitin
SiCHIT
SiCHIT2
Rel. expr. (Chitinase/SiTEF)
0 0.5 1 2 4
Crab shell chitin (mg/mL)

Figure 3: *SiCHIT2* encodes a GH18 chitinase without CBM5 and is expressed during host plant colonization. A) Maximum likelihood tree of all four GH18 chitinases encoded by *Si*. Signal peptides were predicted by SignalP 5.0 and removed prior to amino acid sequence alignment. Amino acid sequences were aligned using the MUSCLE algorithm. A maximum likelihood tree was constructed with 500 bootstraps. A GH18 chitinase from *Plasmodium falciparum* was used as outgroup. Symbols on the right indicate the domain architecture of the full length proteins: small blue box: signal peptide; grey line: inter-domain regions; larger boxes (red, green, blue, beige): GH18 domain; small green box in *Si*CHIT: CBM5. **B)** Amino acid sequence alignment of the catalytic DxxDxDxE motif. Blue: conserved aspartate (D); red: conserved glutamate (E). The asterisk indicates the glutamate that was mutated to glutamin (Q) in the catalytically inactive *Si*CHIT^{E196Q}. **C)** Scheme of the relative location of *SiCHIT* and *SiCHIT2* in the genome of *Si* on contig 0064. The grey bars illustrate introns. *SiCHIT* has 11, and *SiCHIT2* 10 introns. **D, E)** Structure prediction of *Si*CHIT and *Si*CHIT2 by AlphaFold. The sequences of predicted signal peptides were identified with SignalP 5.0 and removed prior to structure prediction. **F)** Expression profile of *SiCHIT* and *SiCHIT2* during confrontation with a bacterial community (SynCom), the pathogen *B. sorokiniana* (*Bs*), or during colonization of the host plants *A. thaliana* (*At*), *B. distachyon* (*Bd*) or *H. vulgare* (*Hv*). The data was taken from Eichfeld *et al.* 2024. **G)** Expression of *SiCHIT* or *SiCHIT2* during *Hv* root colonization at 3, 10 and 21 dpi. Four day old *Hv* roots were inoculated with *Si* and grown on 1/10 PNM medium. Expression was inferred by relative expression of the fungal housekeeping gene *SiTEF* compared to *SiCHIT* or *SiCHIT2* by qPCR using the $2^{-\Delta CT}$ method (mean +/- SD, n = 3-5). **H)** Expression of *SiCHIT* or *SiCHIT2* at six days of growth on 1/10 PNM medium with different fungal species (*Bs* = *Bipolaris sorokiniana*; *Bcs* = *Brunneochlamydosporium sp.*; *Pa* = *Papulaspora equi*; *Po* = *Podospora sp.*; *St* = *Stachybotrys sp.*; *Bj*: *Bjerkandera sp.*; *Mo* = *Mortierella sp.*. Fungal liquid cultures were grown in CM and washed with water, mixed in a 1:1 ratio and 1 g mycelium was streaked out on plates. Expression was inferred by relative expression of the fungal housekeeping gene *SiTEF* compared to *SiCHIT* or *SiCHIT2* by qPCR using the $2^{-\Delta CT}$ method (mean +/- SD, n = 4). **I)** Expression of *SiCHIT* or *SiCHIT2* at six days of growth on crab shell chitin-containing PNM medium at different concentrations. *Si* liquid culture grown in CM was washed with water and 1 g mycelium was streaked out on 1/10 PNM plates. Expression was inferred by relative expression of the fungal housekeeping gene *SiTEF* compared to *SiCHIT* or *SiCHIT2* by qPCR using the $2^{-\Delta CT}$ method (n = 4). Statistical analysis: Statistical analysis: Different letters indicate significant differences according to one-way ANOVA followed by Tukey's HSD test (adjusted p-value < 0.05).

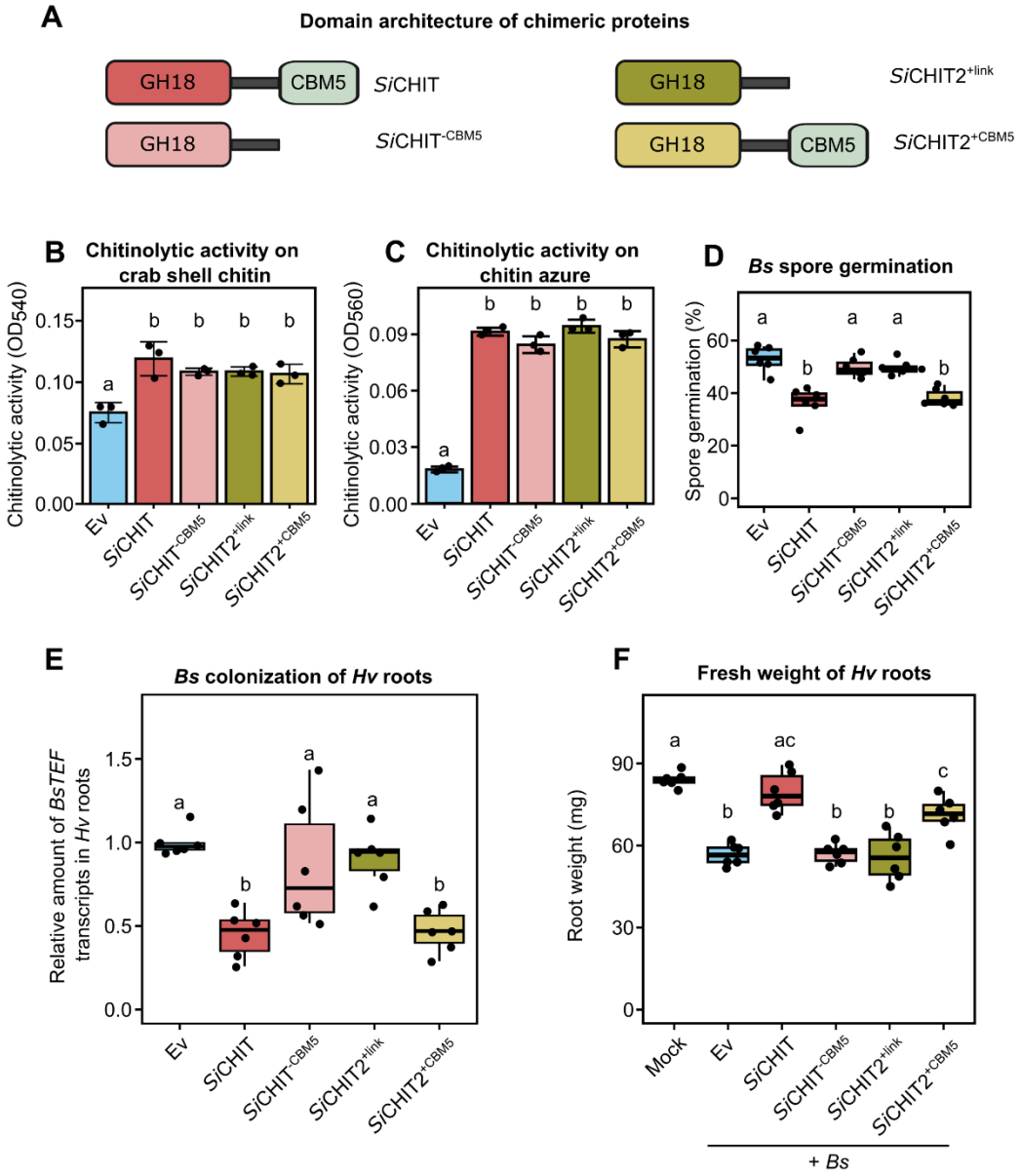

Figure 4: Fusion of the CBM5 to *Si*CHIT2 activates its antifungal and plant-protective capacity. A) Domain architecture of recombinant proteins. *Si*CHIT2^{+link} contains the GH18 domain of *Si*CHIT2 and the linker region of *Si*CHIT. *Si*CHIT2^{+CBM5} contains the GH18 domain of *Si*CHIT2 and the linker region with the CBM5 of *Si*CHIT. **B)** Chitinase activity of recombinant chitinases on crab shell chitin at 10 µM and after 20 h at 28 °C. Samples were spun down and supernatants mixed 1:1 with DNSA reagent. Samples were incubated at 100 °C for 10 min and placed on ice. Subsequently, the relative amount of reducing ends was measured at 540 nm (mean +/- SD, n = 3). **C)** Chitinase activity of recombinant chitinases at 10 µM after 20 h at 28 °C on chitin azure (CA). Samples were spun down and supernatants were quantified at 560 nm (mean +/- SD, n = 3). **D)** Relative *Bs* spore germination six h post incubation in sterile chamber slides with Ev control or 10 µM of *Si*CHIT, *Si*CHIT^{-CBM5}, *Si*CHIT2^{+link} or *Si*CHIT^{+CBM5}. (n = 6). **E)** Colonization of *Hv* roots by *Bs* at three dpi inferred from relative expression of the fungal housekeeping gene *BsTEF* compared to the *Hv* housekeeping gene *HvUBI* by qPCR using the $2^{-\Delta CT}$ method. Colonization values were normalized to the Ev control. *Bs* spores were either pre-treated with the Ev control or 10 µM of recombinant chitinases for 20 h at 28 °C (n = 6). **F)** *Hv* root fresh weight at three dpi with *Bs* spores. *Bs* spores were either pre-

treated with the Ev control or 10 µM of recombinant chitinases for 20 h at 28 °C. Limits of the boxplots represent the 25th–75th percentile, the horizontal line represents the median and the whiskers the minimum/maximum values without outliers (n = 6). Statistical analysis: Different letters indicate significant differences according to one-way ANOVA followed by Tukey's HSD test (adjusted p-value < 0.05).

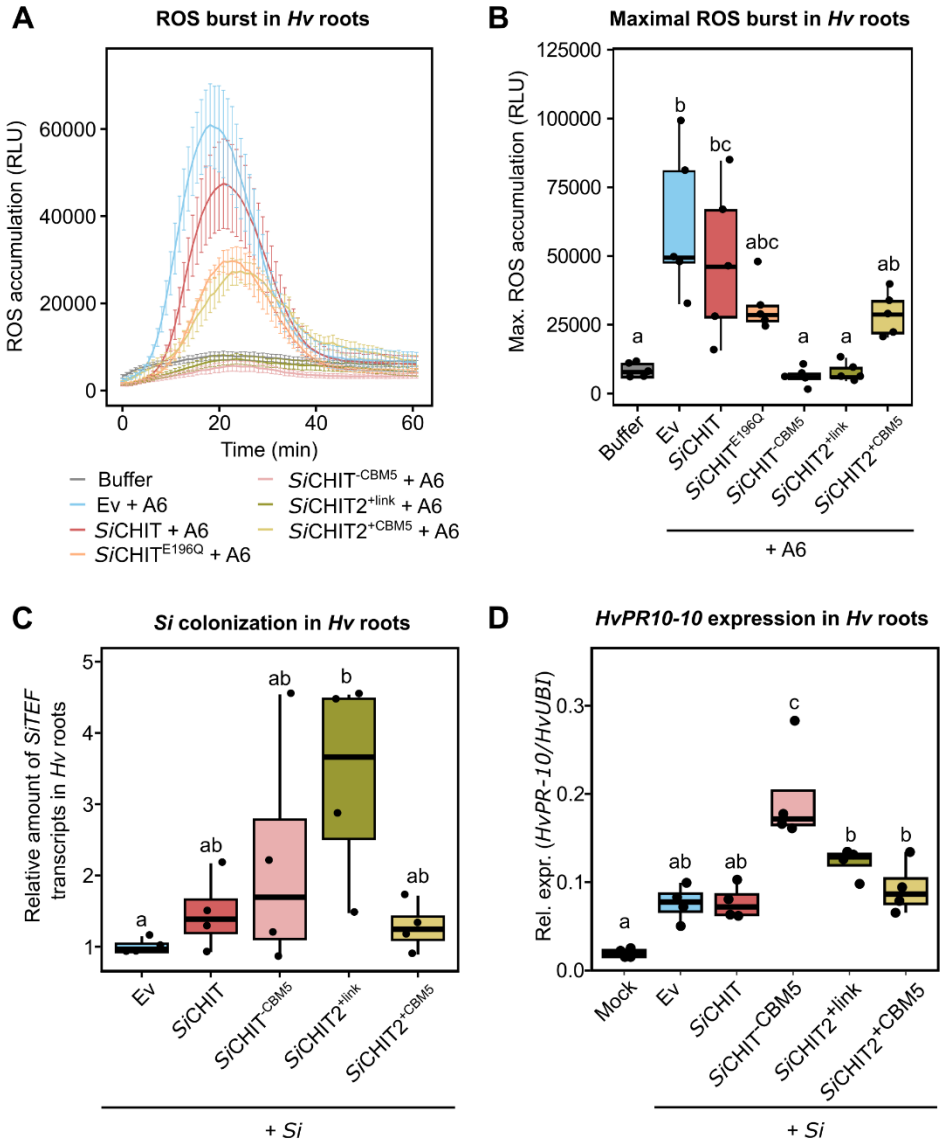

Figure 5: *Si*CHIT2 suppresses chitin-triggered immunity and facilitates root colonization by *Si* in *Hv*. A) ROS burst of 4 d *Hv* roots after treatment with 125 nM chitohexaose (A6). Chitohexaose was incubated with the indicated recombinant chitinases in an equimolar concentration (10 µM) 20 h prior to treatment of *Hv* roots. Values represent means +/- SD from five to six individual wells containing four root pieces of ~ 0.5 cm. **B)** Maximum values of ROS accumulation of *Hv* roots (data from **A**). **C)** Colonization of *Hv* roots by *Si* at three dpi inferred from relative expression of the fungal housekeeping gene *SiTEF* compared to the *Hv* housekeeping gene *HvUBI* by qPCR using the $2^{-\Delta CT}$ method. Colonization values were normalized to the Ev control. *Si* spores were germinated for 16 h at 28 °C and either incubated with the Ev control or 20 µM of recombinant chitinases immediately before *Hv* root inoculation (n = 4). **D)** Transcript accumulation of the *Hv* defense marker gene *Hv*PR10 at three dpi inferred by relative expression of *HvPR10* relative to the *Hv*

housekeeping gene *HvUBI* by qPCR using the $2^{-\Delta CT}$ method (n = 4). Limits of the boxplots represent the 25th–75th percentile, the horizontal line represents the median and the whiskers the minimum/maximum values without outliers. Statistical analysis: Different letters indicate significant differences according to one-way ANOVA followed by Tukey's HSD (adjusted p-value < 0.05).

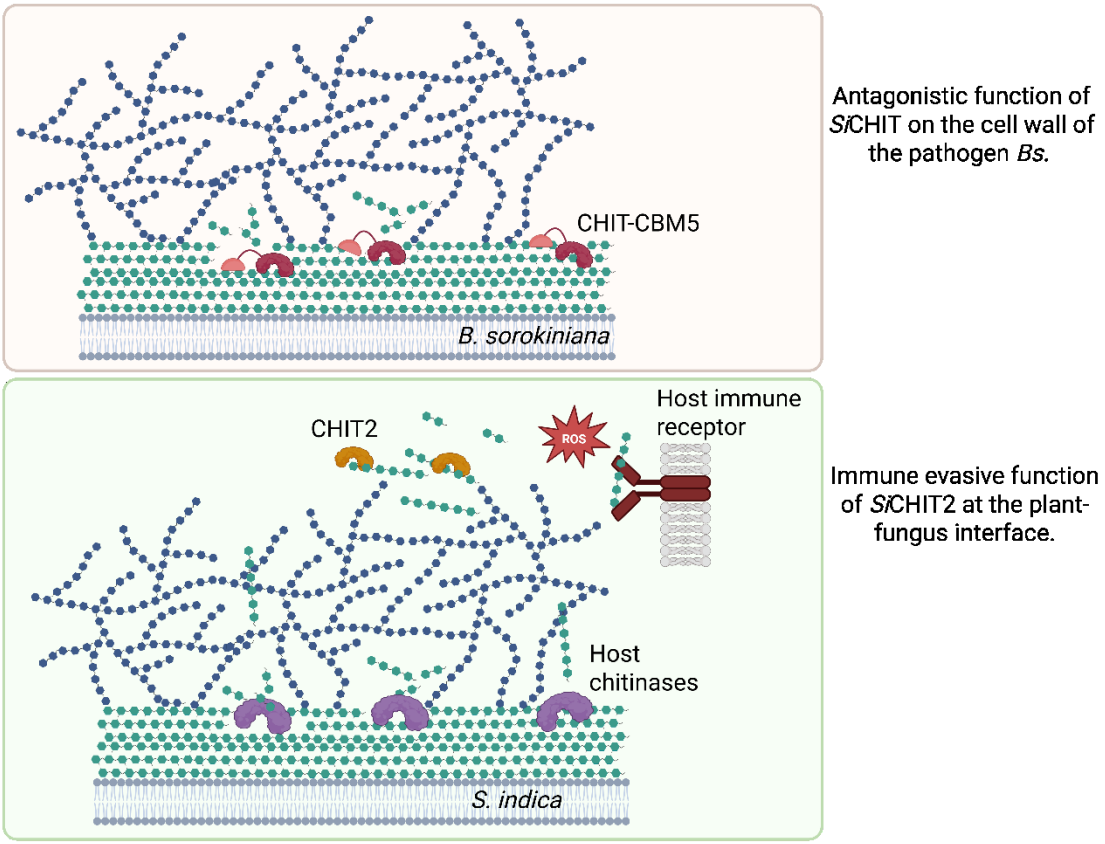

Figure 6: Model displaying the divergent functions of *Si*CHIT and *Si*CHIT2. During confrontation with the pathogen *Bs*, *Si* secretes a GH18-CBM5 chitinase that efficiently inhibits the growth of *Bs*, enabling *Si* to secure its ecological niche. To effectively function in this context, *Si*CHIT relies on the presence of the CBM5. The paralogous *Si*CHIT2 has a catalytically active GH18 domain but no CBM5. It serves *Si* during host colonization by preventing the elicitation of chitin-triggered immunity at the fungus-plant interface, putatively by degrading immunogenic chitin oligomers that are released from the cell wall of *Si* by host chitinases. Figure was created using Biorender.